Stopped-Flow Studies of the Kinetics of Single-Stranded DNA Binding and Wrapping around the *Escherichia coli* SSB Tetramer†

Alexander G. Kozlov and Timothy M. Lohman*

Department of Biochemistry and Molecular Biophysics, Washington University School of Medicine, 660 South Euclid Avenue, St. Louis, Missouri 63110

Received February 12, 2002; Revised Manuscript Received March 21, 2002

ABSTRACT: We have examined the kinetic mechanism for binding of the homotetrameric *Escherichia coli* SSB protein to single-stranded oligodeoxynucleotides [$(dT)_{70}$ and $(dT)_{35}$] under conditions that favor the formation of a fully wrapped ssDNA complex in which all four subunits interact with DNA. Under these conditions, a so-called $(SSB)_{65}$ complex is formed in which either one molecule of $(dT)_{70}$ or two molecules of $(dT)_{35}$ bind per tetramer. Stopped-flow studies monitoring quenching of the intrinsic SSB Trp fluorescence were used to examine the initial binding step. To examine the kinetics of ssDNA wrapping, we used a single-stranded oligodeoxythymidylate, $(dT)_{66}$, that was labeled on its 3′-end with a fluorescent donor (Cy3) and on its 5′-end with a fluorescent acceptor (Cy5). Formation of the fully wrapped structure was accompanied by extensive fluorescence resonance energy transfer (FRET) from Cy3 to Cy5 since the two ends of $(dT)_{66}$ are in close proximity in the fully wrapped complex. Our results indicate that initial ssDNA binding to the tetramer is very rapid, with a bimolecular rate constant, $k_{1,app}$, of nearly 10^9 M^{-1} s^{-1} in the limit of low salt concentration (<0.2 M NaCl, pH 8.1, 25.0 °C), whereas the rate of dissociation is very low at all salt concentrations that were examined (20 mM to 2 M NaCl or NaBr). However, the rate of initial binding and the rate of formation of the fully wrapped complex are identical, indicating that the rate of wrapping of the ssDNA around the SSB tetramer is very rapid, with a lower limit rate of 700 s^{-1}. The implications of this rapid binding and wrapping reaction are discussed.

The *Escherichia coli* single-stranded binding (SSB)[1] protein is an essential component of the replication machinery and is also required for recombination and DNA repair processes (*1*, *2*). It is a member of the class of helix-destabilizing or ssb proteins that bind with high affinity to ssDNA with little sequence specificity and thus stabilize ssDNA intermediates that are generated during DNA metabolic processes (*3*). In addition to its interactions with ssDNA, SSB protein also interacts with DNA polymerase III holoenzyme through direct contacts with the χ subunit (*4*).

The *E. coli* SSB protein is a homotetramer ($4 \times 18\,843$ Da) whose structure (*5*, *6*) and ssDNA properties have been studied extensively (for reviews, see refs *2*, *7*, and *8*). Due to the fact that all four of the SSB subunits can bind ssDNA, the tetramer can bind to ssDNA in multiple binding modes that differ in the number of subunits used to contact the DNA. Two of the major modes of binding are termed the $(SSB)_{65}$ and $(SSB)_{35}$ modes, where the subscript reflects the average number of nucleotides occluded by the tetramer when bound to a single-stranded polynucleotide. In the $(SSB)_{65}$ binding mode, all four subunits contact the ssDNA and ∼65 nucleotides of DNA wrap around the tetramer (*9*−*13*). At equilibrium, this mode is favored at high monovalent salt concentrations (>0.2 M NaCl), but also in solutions containing >50 mM Mg^{2+} (*10*) or micromolar concentrations of polyamines (*14*). However, at low monovalent salt concentrations, the $(SSB)_{35}$ binding mode is favored in which, on average, only two subunits contact the ssDNA.

The SSB tetramer can bind with nearest neighbor cooperativity to long ssDNA; however, the type and magnitude of this cooperativity depend on the binding mode. The highly "unlimited" cooperative binding that results in the formation of long protein clusters on ssDNA and which is generally believed to be important for this general class of DNA binding proteins appears to occur only when the tetramer is bound in the $(SSB)_{35}$ mode (*13*, *15*, *16*). In contrast, the $(SSB)_{65}$ binding mode displays a "limited" type of cooperativity in which protein clusters are limited to the formation of dimers of tetramers (octamers) (*12*, *13*, *17*, *18*).

The relative stabilities of these two major SSB−ssDNA binding modes are highly dependent upon the monovalent salt concentrations (with distinct effects of both cation and anion type), as well as divalent cations, polyamines, pH, and temperature (*9*−*11*, *14*). These two binding modes result from the fact that ssDNA binds to the four subunits of the SSB tetramer with a salt-dependent negative cooperativity (*19*−*21*). This negative cooperativity is most severe under the low-salt conditions where ssDNA binds tightly to the first two subunits, but much more weakly to the second two

† This research was supported by the NIH (Grant R01 GM30498).

* To whom correspondence should be addressed: Department of Biochemistry and Molecular Biophysics, Box 8231, Washington University School of Medicine, 660 S. Euclid Ave., St. Louis, MO 63110. E-mail: lohman@biochem.wustl.edu. Telephone: (314) 362-4393. Fax: (314) 362-7183.

[1] Abbreviations: Tris, tris(hydroxymethyl)aminomethane; EDTA, ethylenediaminetetraacetic acid; SSB, single-stranded binding; ssDNA, single-stranded DNA; FRET, fluorescence resonance energy transfer.

10.1021/bi020122z CCC: $22.00
Published on Web 04/17/2002

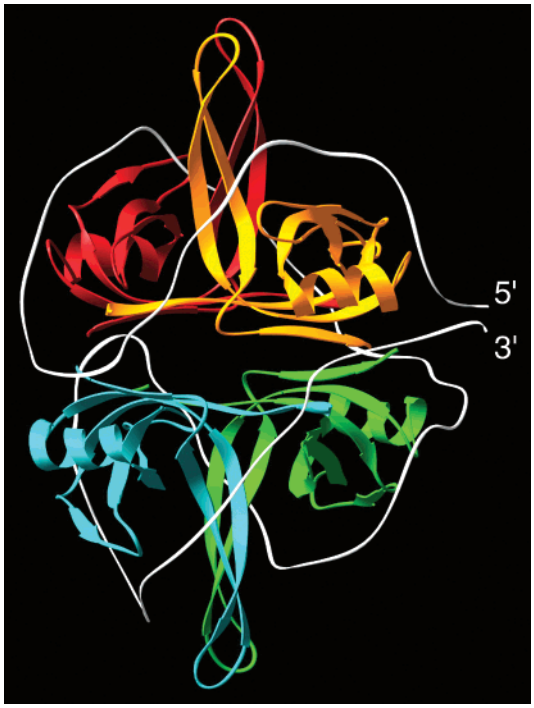

FIGURE 1: Model for the SSB tetramer bound to a ssDNA (white ribbon) of 70 nucleotides in the fully wrapped $(SSB)_{65}$ binding mode, based on the X-ray crystallographic structure of the SSBc tetramer bound to two molecules of $(dC)_{35}$ (*6*).

subunits. Increasing the salt concentration relieves the negative cooperativity significantly, resulting in an increase in the macroscopic ssDNA binding affinity for all four subunits of the tetramer. These salt-dependent changes in negative cooperativity correlate with the salt-dependent transitions between the $(SSB)_{35}$ and $(SSB)_{65}$ polynucleotide binding modes.

High-resolution structural information has recently become available for the *E. coli* SSB_C tetramer (*5*, *22*) and its complex with ssDNA (*6*), as well as for the human mitochondrial SSB tetramer (*23*), which is structurally highly homologous. The SSB_C protein consists of the 135 N-terminal amino acids (42 amino acids were removed from the C-terminus by chymotrypsin treatment) (*24*). This polypeptide contains the ssDNA binding site, still forms stable tetramers, and has the same occluded site size of 65 ± 3 nucleotides per tetramer in the $(SSB)_{65}$ binding mode on poly(dT) (A. G. Kozlov, unpublished data). At NaCl concentrations of >0.2 M, the SSB tetramer forms a 1:1 complex with $(dN)_{70}$, and can bind two molecules of $(dN)_{35}$, although with negative cooperativity (*19*−*21*, *25*). A structure of the SSB_C tetramer in complex with two molecules of $(dC)_{35}$ has been determined at 2.8 Å resolution (*6*). On the basis of this structure, a model for an SSB tetramer−ssDNA complex in the fully wrapped mode has been proposed and is shown schematically in Figure 1. In this structure, 65 nucleotides of ssDNA interact with all four subunits and fully wrap around the SSB tetramer such that the two ends of a 65-nucleotide ssDNA are predicted to enter and exit the tetramer in close proximity. The general topological path of the ssDNA around the tetramer is similar to that followed by the stitching on a baseball.

Although we know a substantial amount about the equilibrium ssDNA binding properties of the *E. coli* SSB tetramer, much less is known about the rates and kinetic mechanisms involved in the formation of these complex structures. What are the relative rates of forming the $(SSB)_{35}$ versus the $(SSB)_{65}$ binding modes? How fast is initial DNA binding relative to formation of a fully wrapped complex? How fast can we expect the SSB tetramer to bind to ssDNA that is transiently formed during DNA replication? To answer these questions, we have undertaken a study of the kinetic mechanism of SSB binding to $(dT)_{70}$ and $(dT)_{35}$ under well-defined conditions such that the final complex formed at equilibrium is a fully wrapped complex with one tetramer bound to one molecule of $(dT)_{70}$ or two molecules of $(dT)_{35}$. The kinetics of these reactions was monitored by stopped-flow techniques using the quenching of the intrinsic Trp fluorescence of the SSB protein upon ssDNA binding, as well as extrinsic fluorescence probes on the ssDNA that allow us to monitor complete wrapping of the ssDNA by fluorescence resonance energy transfer.

MATERIALS AND METHODS

Reagents and Buffers. All solutions were prepared using reagent grade chemicals with distilled water that was further deionized using a Milli Q (Millipore, Bedford, MA) water purification system. Buffer T is 10 mM Tris [tris(hydroxymethyl)aminomethane] and 0.1 mM Na_3EDTA (ethylenediaminetetraacetic acid) at pH 8.1. Buffers were prepared by using 5 M HCl to adjust the pH at 25 °C of solutions of 10 mM Tris base containing the indicated concentrations of NaCl or NaBr.

E. coli SSB Protein and DNA. SSB protein was purified as described previously (*26*), with an additional double-stranded DNA cellulose column to remove a minor exonuclease contaminant (*27*). The SSB protein concentration was determined spectrophotometrically in buffer T with 0.2 M NaCl using an extinction coefficient ϵ_{280} of 1.13×10^5 M^{-1} (tetramer) cm^{-1} (*9*). The SSB protein exists as a stable tetramer at all salt and protein concentrations used in this study (*18*, *28*), and all SSB concentrations are reported for the SSB tetramer. The oligodeoxynucleotides, $(dT)_{70}$ and $(dT)_{35}$, were synthesized using an ABI model 391 automated DNA synthesizer (Applied Biosystems, Foster City, CA) with phosphoramidites from Glenn Research (Sterling, VA). For FRET experiments with 5′-Cy5$(dT)_{65}$Cy3dT-3′, the fluorescent probes Cy5 and Cy3 were incorporated into the DNA at the 5′- and 3′-ends, respectively, using the phosphoramidite forms of the fluorophores. All oligodeoxynucleotides were purified to >99% homogeneity by polyacrylamide gel electrophoresis (PAGE) and electroelution as described previously (*16*). ssDNA concentrations were determined spectrophotometrically in buffer T (pH 8.1) with 0.1 M NaCl using an extinction coefficient ϵ_{260} of 8.1×10^3 M^{-1} (nucleotide) cm^{-1} (*29*) for $(dT)_{35}$ and $(dT)_{70}$. The concentration of Cy5$(dT)_{65}$Cy3dT was determined in buffer T (pH 8.1) with 0.1 M NaCl using an extinction coefficient ϵ_{260} of 5.5×10^5 M^{-1} cm^{-1} (per mole of DNA molecule), which was calculated as the sum of extinction coefficients for oligodeoxythymidylate ($66 \times 8.1 \times 10^3$ M^{-1} cm^{-1}) and Cy3 ($\epsilon_{260} = 5 \times 10^3$ M^{-1} cm^{-1}) and Cy5 ($\epsilon_{260} = 1 \times 10^4$ M^{-1} cm^{-1}) (the latter two supplied by Glenn Research). ssDNA and SSB samples were dialyzed extensively versus buffer T at the indicated salt concentration for use in the stopped-flow kinetic experiments.

Fluorescence Spectra and Titrations. Equilibrium binding of $(dT)_{70}$ to the SSB tetramer was studied by monitoring the quenching of SSB Trp fluorescence, using an SLM 8000C spectrofluorometer [$\lambda_{ex} = 296$ nm (2 nm excitation band-pass) and $\lambda_{em} = 345$ nm (4 nm emission band-pass)] as described previously (*20*, *28*). Fluorescence emission spectra of Cy5$(dT)_{65}$Cy3dT alone and in complex with SSB were recorded using a PTI QM-2000 spectrofluorometer (Photon Technologies, Inc., Lawrenceville, NJ) [$\lambda_{ex} = 515$ nm (2 nm excitation band-pass)] and monitoring the emission from 520 to 800 nm (2 nm emission band-pass). Corrections for the wavelength dependence of the lamp intensity were applied during the recording of the fluorescence spectra using the software provided by the manufacturer.

Fluorescence Stopped-Flow Kinetics. Stopped-flow experiments were performed in buffer T at 25 °C using an Applied Photophysics SX.18MV stopped-flow instrument (Applied Photophysics Ltd., Leatherhead, U.K.) supplied with a 150 W xenon Arc lamp. All optical filters were from Oriel Corp. (Stradford, CT). In experiments for monitoring SSB Trp fluorescence, an excitation wavelength of 296 nm was used and the emission fluorescence was monitored either at wavelengths of >340 nm using a long-pass filter (Oriel catalog no. 51258) or at 350 nm using an interference filter (Oriel catalog no. 53400) as indicated. In experiments for monitoring fluorescence resonance energy transfer (FRET) using fluorescently labeled ssDNA [Cy5$(dT)_{65}$Cy3dT], the Cy3 fluorescence (donor) was excited at 515 nm due to the absence of Cy5 (acceptor) absorbance at this wavelength. The dual-wavelength detection mode of the stopped-flow instrument was used to simultaneously monitor the fluorescence from both the Cy3 donor and the Cy5 acceptor. The fluorescence emission from Cy3 was monitored using a 570 nm interference filter (Oriel catalog no. 53905), and the sensitized fluorescence emission from Cy5 was monitored using a 665 nm long pass filter (Oriel catalog no. 51330). All slit widths were 1.5−2 mm. The reactant solutions were mixed on ice and then incubated in the reservoir syringes of the stopped-flow instrument at 25 °C for at least 5 min prior to mixing. Longer equilibration times had no effect on the results. The concentrations of $(dT)_N$ and SSB reported in the text and plotted in Figures 3, 5, 9, and 10 are the final concentrations after mixing in the stopped-flow instrument.

Analysis of Kinetic Data. All kinetic traces used in the analysis represent an average of 10−14 individual traces. Where applicable, the fluorescence time courses were fit to either one or two exponentials using the Applied Photophysics software or MicroMath (Salt Lake City, UT) Scientist Software according to eq 1

$$F(t) = F_\infty + \sum_{i=1}^{n} A_i \exp(-k_{obs,i}t) \quad (1)$$

where $F(t)$ is the fluorescence intensity at time t, F_∞ is the fluorescence intensity at infinite time, A_i is the amplitude reflecting the ith relaxation process, $k_{obs,i}$ is the observed rate characterizing the ith relaxation process, and $n = 1$ or 2. The uncertainties reported for the observed rates ($k_{obs,i}$) are the standard deviations. Other analyses of the data, including simulations and fitting to appropriate kinetic or equilibrium models, were performed using MicroMath Scientist Software or Mathematica (Wolfram Research, Champaign, IL).

THEORETICAL BACKGROUND

General Analytic Solution for the Kinetic Time Course for a Reversible Bimolecular Association Reaction. For the reversible bimolecular reaction shown in eq 2

$$P + D \underset{k_{-1}}{\overset{k_1}{\rightleftharpoons}} PD \quad (2)$$

where P, D, and PD are the free protein, ssDNA, and protein−DNA complex, respectively, and k_1 and k_{-1} are the bimolecular rate constant and dissociation rate constant, respectively, the differential equation describing the time dependence of [P] is given in eq 3

$$\frac{d[P]}{dt} = -k_1[P][D] + k_{-1}[PD] \quad (3)$$

Using the mass conservation relationships shown in eqs 4

$$[PD] = [P]_{tot} - [P]$$

$$[D] = [D]_{tot} - [PD] = [D]_{tot} - [P]_{tot} + [P] \quad (4)$$

where $[D]_{tot}$ and $[P]_{tot}$ are the total concentrations of DNA and protein, respectively, we can rewrite eq 3 as eq 5

$$\frac{d[P]}{a[P]^2 + b[P] + c} = dt \quad (5)$$

where $a = -k_1$, $b = -[k_{-1} + k_1([D]_{tot} - [P]_{tot})]$, and $c = k_{-1}[P]_{tot}$. Upon integrating eq 5 from $[P] = [P]_{tot}$ at time zero to $[P] = [P]_t$ at time t, we can write the resulting expression in the form of eq 6

$$C = C_0 \exp(\alpha t) \quad (6)$$

where α, C, and C_0 are defined in eqs 7.

$$\alpha = \sqrt{4k_1k_{-1}[P]_{tot} + [k_{-1} + k_1([D]_{tot} - [P]_{tot})]^2} \quad (7a)$$

$$C = \frac{2k_1[P]_t + [k_{-1} + k_1([D]_{tot} - [P]_{tot})] + \alpha}{2k_1[P]_t + [k_{-1} + k_1([D]_{tot} - [P]_{tot})] - \alpha} \quad (7b)$$

$$C_0 = \frac{2k_1[P]_{tot} + [k_{-1} + k_1([D]_{tot} - [P]_{tot})] + \alpha}{2k_1[P]_{tot} + [k_{-1} + k_1([D]_{tot} - [P]_{tot})] - \alpha} \quad (7c)$$

A similar analytic solution of eq 3 has previously been presented by Erickson et al. (*30*), although in a form different from that presented here.

In general, if there is a fluorescence signal change associated with formation of the complex, this can be related to the concentrations of the fluorescent species. For example, the quenching of the SSB (P) Trp fluorescence that occurs upon formation of the SSB−ssDNA complex (PD) can be related to the free protein concentration, $[P]_t$, as in eq 8

$$[F(t) - F_\infty]/(F_0 - F_\infty) = [P]_t/[P]_{tot} \quad (8)$$

where F_0 and F_∞ are the initial fluorescence at time zero and infinite time, respectively, and $F(t)$ is the fluorescence

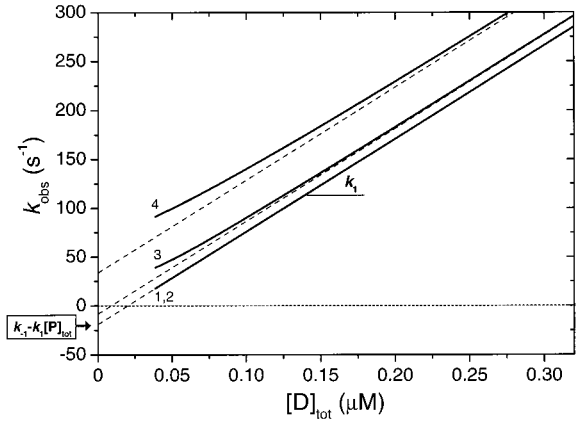

FIGURE 2: Simulated dependencies of the observed rate ($k_{obs} = \alpha$) on $[D]_{tot}$ for a simple bimolecular reaction (see eq 2) calculated according to eq 7a for the following: $[P]_{tot} = 20$ nM, $k_1 = 9.5 \times 10^8$ M^{-1} s^{-1}, and (1) $k_{-1} = 0.01$ s^{-1}, (2) $k_{-1} = 1$ s^{-1}, (3) $k_{-1} = 10$ s^{-1}, and (4) $k_{-1} = 50$ s^{-1} (solid lines). Dashed lines represent the linear extrapolations of the curves from the linear regions that exist at $[D]_{tot} \gg [P]_{tot}$. The slopes of these linear regions yield k_1 and the intercept, which can have a negative value when given by the term $k_{-1} - k_1[P]_{tot}$.

at time t. An explicit expression for the free protein concentration $[P]_t$ can be obtained from eq 6. Introduction of this into eq 8, followed by some rearrangement, yields eq 8a.

$$F(t) = F_\infty + (F_0 - F_\infty) \times \frac{C_0 \exp(\alpha t)[k_{-1} + k_1([D]_{tot} - [P]_{tot}) - \alpha] - [k_{-1} + k_1([D]_{tot} - [P]_{tot}) + \alpha]}{2k_1[P]_{tot}[1 - C_0 \exp(\alpha t)]} \quad (8a)$$

Therefore, nonlinear least-squares analysis can be used to fit any fluorescence time trace, $F(t)$, that was monitored at particular $[P]_{tot}$ and $[D]_{tot}$ values, to eq 8a to obtain F_0, F_∞, k_1, and k_{-1}.

Under conditions such that $[D]_{tot} \gg [P]_{tot}$ and $k_1[D]_{tot} \gg k_{-1}$, eq 6 simplifies to eq 9

$$\frac{C}{C_0} = \exp(\alpha t) \approx \frac{[P]_{tot}}{[P]} \quad (9)$$

which can be rewritten as eq 10.

$$[P] = [P]_{tot} \exp(-\alpha t) \quad (10)$$

Therefore, under these conditions ($[D]_{tot} \gg [P]_{tot}$ and $k_1[D]_{tot} \gg k_{-1}$), the time-dependent change in the free protein concentration ([P]) will follow a single-exponential decay with an observed rate k_{obs} ($=\alpha$). This observed rate depends on the total ssDNA concentration, $[D]_{tot}$, as in eq 7a, which can be simplified to the expression in eq 11 when $[D]_{tot} \gg [P]_{tot}$.

$$k_{obs} = k_{-1} - k_1[P]_{tot} + k_1[D]_{tot} \quad (11)$$

Under these conditions, a plot of k_{obs} versus $[D]_{tot}$ will be linear with a slope equal to k_1 and an intercept equal to $k_{-1} - k_1[P]_{tot}$. Figure 2 shows a series of plots (solid lines) of k_{obs} versus $[D]_{tot}$ generated using eq 7a for a $[P]_{tot}$ of 20 nM and a $[D]_{tot}$ ranging from ~40 to ~300 μM with a k_1 of 9.5×10^8 M^{-1} s^{-1} and k_{-1} values of 0.01, 1, 10, and 50 s^{-1}. The dashed lines in Figure 2 show linear extrapolations of the plots to a $[D]_{tot}$ of 0.

Two interesting conclusions can be drawn from the above analysis. The first is that when $k_1[D]_{tot} \gg k_{-1}$ one can observe a negative intercept in a plot of k_{obs} versus $[D]_{tot}$ due to the dominance of the $-k_1[P]_{tot}$ term over the k_{-1} term in eq 11. When the value of k_{-1} is increased, the intercept will eventually shift to a positive value. The second conclusion is that a reliable estimate of k_1 can be obtained from a plot of k_{obs} versus $[D]_{tot}$ even for data obtained at fairly low $[D]_{tot}$:$[P]_{tot}$ ratios (e.g., for $[D]_{tot}$:$[P]_{tot}$ ratios of <10). For example, if $k_1/k_{-1} = 10^9$ M^{-1}, as is the case for all of our experiments, with the exception of those performed in 2 M NaBr (see Table 1), the values of k_1 estimated from the slope, $dk_{obs}/d[D]_{tot}$ (see eq 7a), are only 2 and 7% lower than the input value for simulations performed at $[P]_{tot} = 20$ nM and $[D]_{tot} = 60$ and 40 nM, respectively. These deviations further decrease with increasing $[P]_{tot}$ or $[D]_{tot}$ values. Therefore, under these conditions, reliable estimates of k_1 can be obtained from the slope even for $[D]_{tot}$:$[P]_{tot}$ ratios of ~2−3. This latter conclusion was further corroborated by comparing the values of k_{obs} ($=\alpha$) predicted from eq 7a with the values of k_{obs} obtained from single-exponential fits (eq 1) of time traces ($[P]_t$) rigorously simulated according to eq 6 for $[D]_{tot}$:$[P]_{tot} \geq 2$ and $k_1[D]_{tot} \gg k_{-1}$.

RESULTS

Kinetics of the Binding of the SSB Tetramer to $(dT)_{70}$. It has been shown in equilibrium binding studies (*20*, *21*) and by isothermal titration calorimetry (ITC) (*25*) that at monovalent salt concentrations above 0.2 M the SSB tetramer binds $(dT)_{70}$ with a 1:1 stoichiometry with very high affinity. Under these conditions, $(dT)_{70}$ interacts with all four subunits of the SSB tetramer wrapping around the outside of the tetramer (*2*, *9*, *12*, *13*). Figure 1 shows a structural model for this fully wrapped binding mode, based on the X-ray crystallographic structure of two molecules of $(dC)_{35}$ bound to the SSB_C tetramer, in which 42 amino acids have been deleted from the C-terminus of each subunit (*6*). In this structure, the ssDNA follows a path that resembles that of the stitching on a baseball or tennis ball. The maximum Trp fluorescence quenching associated with SSB binding to $(dT)_{70}$ in this binding mode is ~90% at equilibrium (*20*, *21*).

The kinetics of this interaction was examined by performing a series of stopped-flow experiments in 0.2 M NaCl (buffer T, pH 8.1, 25.0 °C) by mixing SSB protein (at either 20 or 100 nM tetramer) with $(dT)_{70}$ at concentrations ranging from 20 nM to 1 μM. The progress of the reaction was monitored by the quenching of the SSB Trp fluorescence upon complex formation. Under these conditions, the final product is a 1:1 complex in which all four SSB subunits interact with the bound $(dT)_{70}$.

Figure 3A shows a series of time courses performed at 20 nM SSB tetramer and $(dT)_{70}$ concentrations of 40, 100, 150, and 300 nM (buffer T, pH 8.1, 0.2 M NaCl, 25.0 °C). Each time course shows a single-exponential decrease in Trp fluorescence that approaches the same plateau value corresponding to approximately 84−86% quenching of the initial SSB fluorescence, in reasonable agreement with the maximum fluorescence quenching of 90% that is observed upon titration of SSB with $(dT)_{70}$ under the same conditions at equilibrium (*21*). This suggests that the time course reflects formation of the fully wrapped SSB−$(dT)_{70}$ complex. As expected, the rates of fluorescence quenching increase with

Table 1: Equilibrium and Kinetic Constants for SSB Binding to $(dT)_{70}$ at Different NaBr and NaCl Concentrations (monitoring SSB Trp fluorescence)[a]

[NaBr] (M)	K_{obs}[b] (M^{-1}), equil. titration	$k_{1,app}$ (M^{-1} s^{-1}), slope	$k_{1,app}$ (s^{-1}), direct fit (1:1)	intercept (s^{-1})	$k_{-1,app}$ (s^{-1}), $k_{1,app}/K_{obs}$	$k_{-1,app}$ (s^{-1}), direct fit (1:1)
0.2	–	$(6.82 \pm 0.06) \times 10^8$	$(6.72 \pm 0.03) \times 10^8$	-9.7 ± 1.0	–	0.0059 ± 0.0007
0.4	–	$(3.71 \pm 0.03) \times 10^8$	$(3.50 \pm 0.01) \times 10^8$	-5.1 ± 0.7	–	0.0117 ± 0.0006
1.0	$(2.67 \pm 0.20) \times 10^9$	$(1.18 \pm 0.01) \times 10^8$	$(1.09 \pm 0.01) \times 10^8$	-1.1 ± 0.5	0.044 ± 0.003	0.0085 ± 0.0003
1.0[b]			$(1.21 \pm 0.01) \times 10^8$			0.0096 ± 0.0013
1.2	$(8.07 \pm 0.34) \times 10^8$	$(9.09 \pm 0.06) \times 10^7$	$(8.92 \pm 0.05) \times 10^7$	-0.4 ± 0.4	0.11 ± 0.01	0.050 ± 0.001
2.0	$(2.74 \pm 0.12) \times 10^7$	$(4.24 \pm 0.03) \times 10^7$	–	1.85 ± 0.40	1.55 ± 0.07	1.60 ± 0.03

[NaCl] (M)	K_{obs} (M^{-1}), equil. titration	$k_{1,app}$ (M^{-1} s^{-1}), slope	$k_{1,app}$ (M^{-1} s^{-1}), direct fit (1:1)	intercept (s^{-1})	$k_{-1,app}$ (s^{-1}), $k_{1,app}/K_{obs}$	$k_{-1,app}$ (s^{-1}), direct fit (1:1)
0.02	–	$(1.13 \pm 0.03) \times 10^9$	–	-14.3 ± 4.4	–	–
0.2	–	$(9.47 \pm 0.30) \times 10^8$	$(9.30 \pm 0.11) \times 10^8$	-9.2 ± 6.7	–	0.052 ± 0.016
0.2[b]		$(9.29 \pm 0.03) \times 10^8$	$(9.07 \pm 0.05) \times 10^8$	-67 ± 11		0.044 ± 0.004
1.0	–	$(2.76 \pm 0.02) \times 10^8$	$(2.50 \pm 0.01) \times 10^8$	-4.6 ± 0.8	–	0.040 ± 0.001
1.0[c]		$(2.93 \pm 0.06) \times 10^8$	$(2.82 \pm 0.03) \times 10^8$	-4.9 ± 1.3		0.058 ± 0.003
1.0[d]		$(2.65 \pm 0.06) \times 10^8$	$(2.52 \pm 0.01) \times 10^8$	-1.9 ± 1.2		0.029 ± 0.001
1.2	–	$(2.33 \pm 0.01) \times 10^8$	$(2.20 \pm 0.05) \times 10^8$	-4.0 ± 0.4	–	0.0026 ± 0.0001
2.0	–	$(1.31 \pm 0.01) \times 10^8$	$(1.23 \pm 0.01) \times 10^8$	-2.0 ± 0.6	–	0.0088 ± 0.0002

[a] Conditions: buffer T, pH 8.1, 25 °C. [b] The concentration of SSB used in these experiments was 0.1 μM. [c] Cy5$(dT)_{65}$Cy3dT was used in these experiments. [d] The Cy5 FRET fluorescence from Cy5$(dT)_{65}$Cy3dT was used to monitor binding by an excess of SSB.

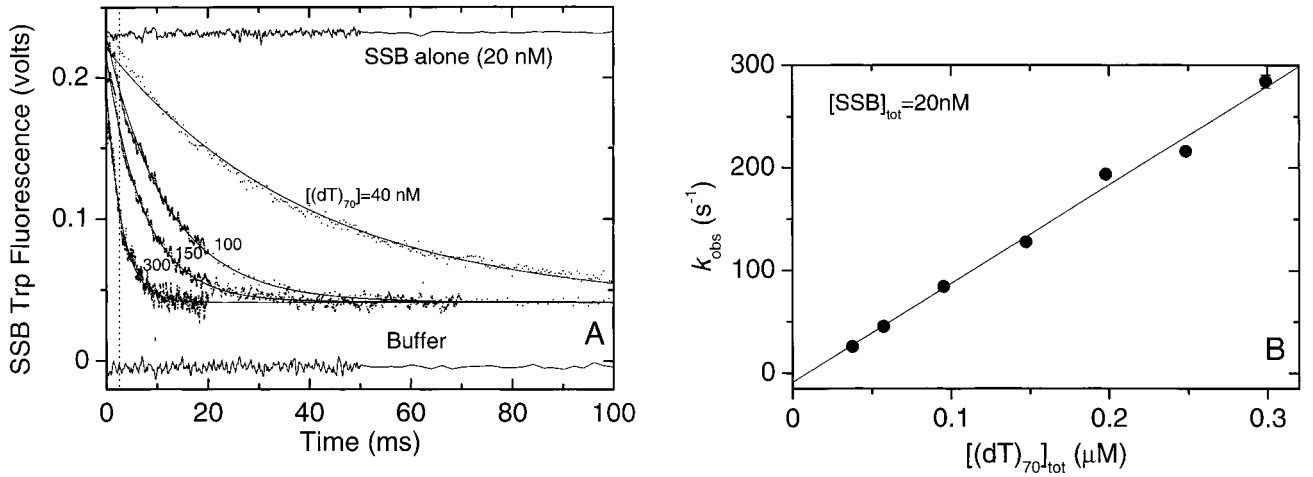

FIGURE 3: Stopped-flow kinetic time courses for $(dT)_{70}$ binding to SSB, monitored by the quenching of the SSB Trp fluorescence. (A) Kinetic traces were obtained by mixing 20 nM SSB (20 nM tetramer) with varying concentrations of $(dT)_{70}$ (40, 100, 150, and 300 nM) (0.2 M NaCl, buffer T, pH 8.1, 25 °C). Solid lines are the best fits of the traces to single-exponential functions to obtain k_{obs} using eq 1. Only data points to the right of the vertical line corresponding to 2.5 ms were used in the analyses to avoid any possible artifacts arising from the dead time of the instrument (~2 ms). (B) Observed rates (k_{obs}) obtained from the single-exponential fits of the time courses in panel A plotted as a function of $[(dT)_{70}]_{tot}$. The solid line is the linear least-squares fit of the data which yields a slope $k_{1,app}$ of $(9.47 \pm 0.30) \times 10^8$ s^{-1} M^{-1} and a negative intercept of -9.2 ± 6.7 s^{-1}.

increasing $(dT)_{70}$ concentration. The traces in Figure 3A were fit to single-exponential decays using eq 1 to obtain values of k_{obs} at each $(dT)_{70}$ concentration. The single-exponential fits are good starting at $[dT_{70}]_{tot}$:$[SSB]_{tot}$ ratios of ≥ 2. Only data points to the right of the vertical line corresponding to 2.5 ms were used in fitting to avoid any possible artifacts arising from the dead time of the instrument (~2 ms). The values of k_{obs} obtained from this analysis are plotted as a function of $[(dT)_{70}]_{tot}$ in Figure 3B.

Figure 3B shows that under these pseudo-first-order conditions ($[(dT)_{70}]_{tot} > [SSB]_{tot}$) the observed rate increases linearly with increasing $[(dT)_{70}]_{tot}$ from ~26 s^{-1} [40 nM $(dT)_{70}$] to ~284 s^{-1} [300 nM $(dT)_{70}$]. The linear least-squares line in Figure 3B has a slope k_1 of $(9.47 \pm 0.30) \times 10^8$ M^{-1} s^{-1} and an intercept of -9.2 ± 6.7 s^{-1}. This negative intercept is real and indicates that $k_1[P]_{tot} \gg k_{-1}$ (see eq 11), and the experimental line agrees well with curve 1 in Figure 2 that was simulated using eq 7a with a k_1 of 9.5×10^8 M^{-1} s^{-1}, a k_{-1} of 0.01 s^{-1}, and a $[P]_{tot}$ of 20 nM.

A stopped-flow SSB Trp fluorescence time course obtained upon mixing the SSB tetramer with $(dT)_{70}$ at a 1:1 molar ratio {$[SSB]_{tot} = 20$ nM and $[(dT_{70})]_{tot} = 19.3$ nM} is shown in Figure 4. This time course was analyzed by directly fitting it to the analytic solution for a 1:1 reversible reaction (eq 8a, solid line in Figure 4) to obtain estimates of k_1 and k_{-1}. The best fit parameters determined from this analysis are as follows: $k_1 = (9.30 \pm 0.11) \times 10^8$ M^{-1} s^{-1}, $k_{-1} = 0.052 \pm 0.016$ s^{-1}, $F_0 = 0.247 \pm 0.001$, and $F_\infty = 0.047 \pm 0.001$ (residuals for this fit shown in Figure 4). Also shown in Figure 4 is the best fit of a single exponential (dashed line) to the same data, which clearly does not describe the time course as well. For the remainder of our discussion, we will refer to the experimentally determined values of the kinetic rate constants as $k_{1,app}$ and $k_{-1,app}$.

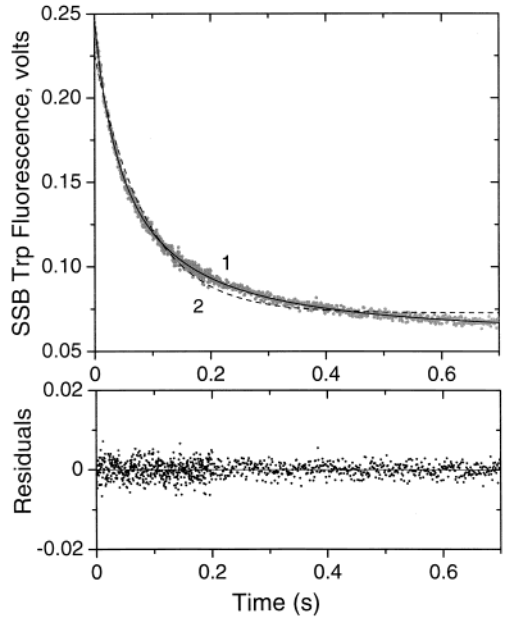

FIGURE 4: Kinetic time course obtained upon mixing equimolar concentrations of SSB tetramer with $(dT)_{70}$. A stopped-flow experiment was performed by mixing SSB protein (20 nM tetramer) with $(dT)_{70}$ (19.3 nM) while monitoring the SSB Trp fluorescence (gray circles). The smooth line (1) shows the nonlinear least-squares fit of the data to eq 8a yielding the following values: $F_0 = 0.247 \pm 0.001$, $F_\infty = 0.047 \pm 0.001$, $k_1 = (9.30 \pm 0.11) \times 10^8$ M^{-1} s^{-1}, and $k_{-1} = 0.052 \pm 0.016$ s^{-1}. The residuals for this fit are shown in the bottom panel. For comparison, the dashed line shows the best fit of these same data to a single-exponential function (eq 1) where $A = 0.153 \pm 0.001$, $k_{obs} = 11.5 \pm 0.1$, and $F_\infty = 0.073 \pm 0.001$, which does not provide a good description of the time course under these conditions.

Scheme 1

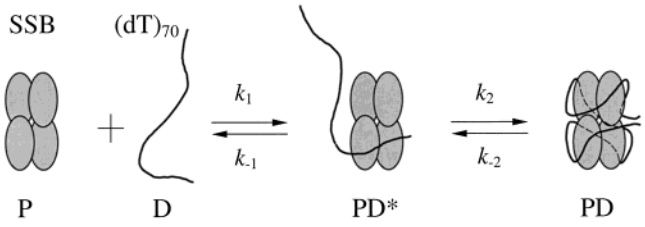

The value of the apparent bimolecular association rate constant $[(9.30 \pm 0.11) \times 10^8$ M^{-1} $s^{-1}]$ obtained from the fit to the fluorescence time course shown in Figure 4 agrees well with the value $[k_{1,app} = (9.47 \pm 0.30) \times 10^8$ s^{-1} $M^{-1}]$ obtained from the slope of a plot of k_{obs} versus $[D]_{tot}$ under pseudo-first-order conditions. However, it is important to mention that the value of $k_{-1,app}$ obtained from the fit (see Table 1) does not likely reflect a true dissociation rate constant but rather is a composite of several rate constants if the binding process actually involves multiple steps. In fact, this appears to be the case since we have evidence for an additional fast step involving wrapping of ssDNA around the SSB tetramer (see Scheme 1 and the Discussion).

Experiments similar to those described above (buffer T, pH 8.1, 0.2 M NaCl, 25.0 °C) were also performed at a 5-fold higher total SSB concentration (100 nM). The results obtained from analysis of these data performed under pseudo-first-order conditions ($[D]_{tot} \gg [P]_{tot}$) as well as by direct fitting of the traces obtained for experiments performed when $[(dT)_{70}]_{tot} \approx [SSB]_{tot}$ are summarized in Table 1 and are in very good agreement with the values of $k_{1,app}$ and $k_{-1,app}$ obtained for the experiments performed at 20 nM SSB (see Table 1).

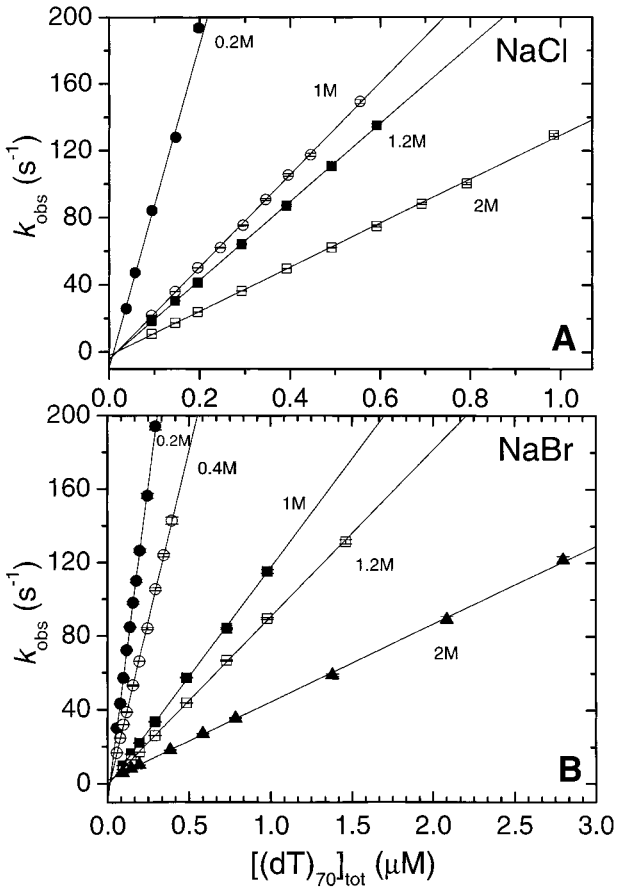

FIGURE 5: Effect of monovalent salt concentration and type on the dependence of the observed rate (k_{obs}) on $[(dT)_{70}]_{tot}$ for SSB binding to $(dT)_{70}$. (A) Effect of [NaCl] (buffer T, pH 8.1, 25 °C). (B) Effect of [NaBr] (buffer T, pH 8.1, 25 °C). The values of k_{obs} were obtained from nonlinear least-squares fits to a single-exponential function (eq 1) of stopped-flow time courses monitoring the Trp fluorescence quenching of SSB protein (20 nM tetramer) performed at different $(dT)_{70}$ concentrations.

Effects of Monovalent Salt Concentration on the Kinetics of the SSB Tetramer Binding to $(dT)_{70}$. We next examined the effects of monovalent salt concentration (from 0.2 to 2 M NaCl and NaBr) on the kinetics of SSB binding to $(dT)_{70}$ by monitoring the SSB Trp fluorescence quenching upon complex formation (buffer T, pH 8.1, 25.0 °C). Results of experiments performed under pseudo-first-order conditions $\{[SSB]_{tot} = 20$ nM, $[(dT)_{70}] = 40$ nM $- 3$ μM$\}$ were analyzed by fitting the time courses to single-exponential functions and plotting k_{obs} versus $[(dT)_{70}]$. Results of experiments performed at equimolar concentrations of SSB and $(dT)_{70}$ were analyzed by fitting the complete time courses directly to eq 8a.

The results of the experiments performed under pseudo-first-order conditions are shown in Figure 5. At all salt concentrations, k_{obs} increases linearly with increasing $[(dT)_{70}]_{tot}$. The values of $k_{1,app}$ obtained from the slopes of these plots are consistent with the values obtained from direct fitting to eq 8a (see Table 1). The values of $k_{1,app}$ are plotted as a function of [NaCl] and [NaBr] in Figure 6 and are observed to decrease with increasing salt concentration. The value of $k_{1,app}$ appears to reach a plateau value of $\sim 10^9$ M^{-1} s^{-1} below

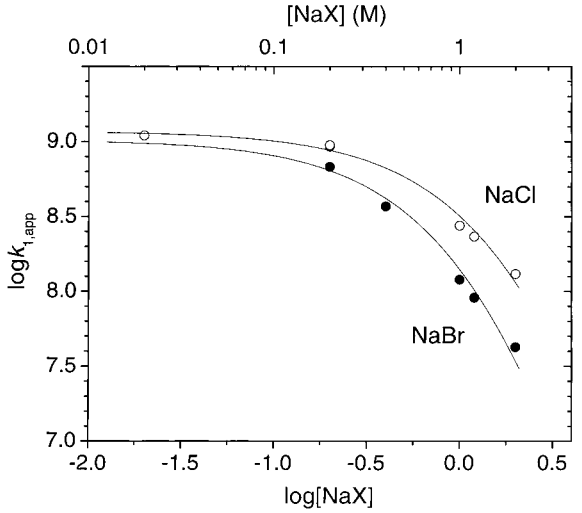

FIGURE 6: Dependence of the apparent bimolecular association rate constant ($k_{1,app}$) on monovalent salt concentration and type for the binding of $(dT)_{70}$ to the SSB tetramer. Values of log $k_{1,app}$ (determined from the plots in Figure 5) are plotted versus log[NaCl] (○) and log[NaBr] (●) (buffer T, pH 8.1, 25 °C). Solid lines are nonlinear least-squares fits of the data to eq 16 with a fixed value for n of 5 and the following parameters: $k_{1,0} = (1.17 \pm 0.09) \times 10^9$ M^{-1} s^{-1} and $K_{Cl} = 0.30 \pm 0.02$ M^{-1} for the data obtained in NaCl, and $k_{1,0} = (1.02 \pm 0.13) \times 10^9$ M^{-1} s^{-1} and $K_{Br} = 0.49 \pm 0.04$ M^{-1} for the data obtained in NaBr.

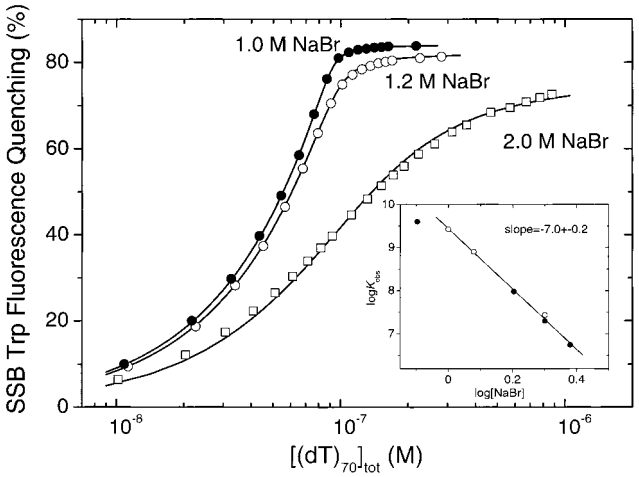

FIGURE 7: Equilibrium isotherms for SSB tetramer binding to $(dT)_{70}$ as a function of [NaBr]. Titrations performed at 0.1 μM SSB tetramer were monitored by the quenching of the SSB Trp fluorescence upon titration with $(dT)_{70}$ (buffer T, pH 8.1, 25 °C) in the presence 1 (●), 1.2 (○), and 2 M NaBr (□). The solid lines are the best fits to a single-site binding model, yielding the equilibrium binding constants, K_{obs}, given in Table 1. The inset shows a plot of log K_{obs} (○) vs log[NaBr] [(●) data from ref *20*].

0.2 M NaCl, but decreases above 0.2 M NaCl, reaching a value of $\sim 10^8$ M^{-1} s^{-1} at 2.0 M NaCl. It is also obvious that the values of $k_{1,app}$ are consistently lower in NaBr than in NaCl, in the range from 0.2 to 2 M, where comparisons were available. However, the differences in $k_{1,app}$ become less at lower NaCl and NaBr concentrations. In the high-salt region (1−2 M), the limiting values of d(log $k_{1,app}$)/d(log[NaCl]) and d(log k_1)/d(log[NaBr]) are −1.1 and −1.5, respectively. All rate constants determined are summarized in Table 1.

Comparisons of Equilibrium and Kinetic Data for $(dT)_{70}$−SSB Binding at High NaBr Concentrations. Although the equilibrium binding affinity of SSB for $(dT)_{70}$ is salt sensitive, the equilibrium binding affinity of the SSB tetramer for $(dT)_{70}$ is very high in NaCl salts, in fact too high to measure, even using fluorescence techniques, at all concentrations of SSB, $(dT)_{70}$, and NaCl used in this study (*21*, *25*). Binding of SSB to $(dT)_{70}$ is stoichiometric even at 3 M NaCl. However, the affinity of SSB for $(dT)_{70}$ is lower and can be measured accurately at NaBr concentrations of >1 M, and the affinity decreases with increasing NaBr concentration (*20*). We therefore performed equilibrium binding studies of the SSB−$(dT)_{70}$ interaction at several high NaBr concentrations used in our kinetic studies to compare the kinetic rate constants determined with accurate measurements of the equilibrium constants.

Figure 7 shows a series of equilibrium binding isotherms obtained by titrating solutions of SSB (100 nM) with $(dT)_{70}$ in the presence of 1, 1.2, and 2 M NaBr (buffer T, pH 8.1, 25 °C). The isotherms were fit to a 1:1 binding model, and the equilibrium binding constant, K_{obs}, was determined from a nonlinear least-squares fit to the data. The values of K_{obs} determined from these fits are listed in Table 1 and plotted as log K_{obs} versus log[NaBr] in the inset of Figure 7 (○), along with values of K_{obs} determined previously (*20*). K_{obs} decreases with increasing NaBr concentration such that d(log K_{obs})/d(log[NaBr]) = −7.0 ± 0.2. As shown in the inset to Figure 7, the values of K_{obs} determined here agree well with those determined previously (*20*).

Using these equilibrium constants and the values of the bimolecular association rate constants, $k_{1,app}$, determined under the same solution conditions (Table 1), we can obtain estimates of the apparent dissociation rate constants, $k_{-1,app}$, by assuming that the reaction occurs in a single step such that $k_{-1,app} = k_{1,app}/K_{obs}$. Although this is certainly not the case, and thus the values of $k_{-1,app}$ should not be considered to be elementary rate constants, they provide estimates of the macroscopic dissociation rate constants, and thus some estimates of the apparent lifetimes of these complexes.

The values of $k_{-1,app}$ estimated from the $k_{1,app}/K_{obs}$ ratio are 0.044 ± 0.003, 0.11 ± 0.01, and 1.55 ± 0.07 s^{-1} at 1.0, 1.2, and 2.0 M NaBr, respectively (Table 1, column 6). Therefore, $k_{-1,app}$ is quite low for each of these NaBr concentrations, but increases with increasing salt concentration, as expected (*31*) such that d(log $k_{-1,app}$)/d(log[NaBr]) = 5.4 ± 0.3. The values of $k_{-1,app}$ estimated here are small and thus difficult to measure using the approaches discussed here. However, the value of $k_{-1,app}$ estimated at 2 M NaBr as $k_{1,app}/K_{obs} = 1.55 \pm 0.07$ s^{-1} compares well with the value of $k_{-1,app}$ (1.60 ± 0.03 s^{-1}) determined from a direct fit of the time course to eq 8a (see Table 1).

Kinetics of SSB Binding to Cy5$(dT)_{65}$Cy3dT, Monitored by Changes in FRET. The stopped-flow kinetic studies reported above in which SSB tetramer binding to $(dT)_{70}$ was monitored by the quenching of the SSB Trp fluorescence indicate that formation of the fully wrapped complex can be described by a single-step reaction occurring with a very fast apparent bimolecular rate constant approaching 1×10^9 M^{-1} s^{-1} at low NaCl concentrations, which is very near the rate expected for a diffusion-controlled reaction (see the Discussion). Certainly, the formation of the fully wrapped structure must occur in multiple steps, although some of those steps may be sufficiently fast such that the reaction appears to occur in a single step. However, changes in the SSB Trp

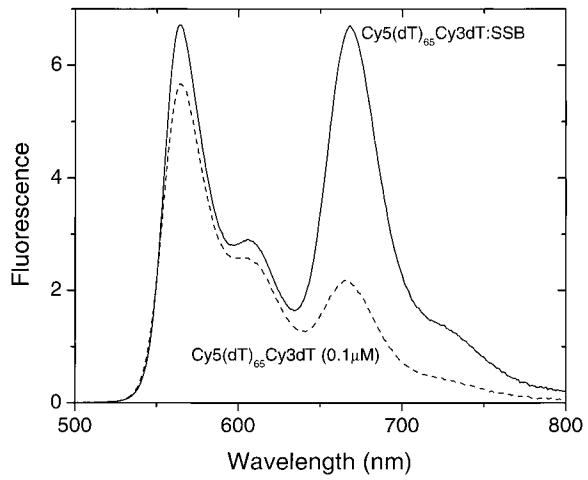

FIGURE 8: Fluorescence emission spectra of Cy5$(dT)_{65}$Cy3dT (0.1 μM, dashed line) and a 1:1 mixture of Cy5$(dT)_{65}$Cy3dT and SSB (both at 0.1 μM, solid line; buffer T, pH 8.1, 1.0 M NaCl, 25 °C). An excitation wavelength of 515 nm was used to record the spectra, which excites only the Cy3 (donor) fluorescence. These show the increase in fluorescence resonance energy transfer (FRET) from the Cy3 donor fluorophore to the Cy5 acceptor fluorophore upon binding of the SSB tetramer in the fully wrapped complex (see Figure 1). The Cy3 fluorescence has its peak at 565 nm, whereas the Cy5 fluorescence has its peak at 667 nm. Each spectrum was corrected for the wavelength dependence of the excitation lamp intensity.

fluorescence are expected to occur during both the binding step and the ssDNA wrapping step, and thus, this is not the best probe to attempt to differentiate between these two processes. To attempt to differentiate the initial ssDNA binding step from the ssDNA wrapping step, we designed a fluorescently labeled ssDNA molecule that should mainly be sensitive to the formation of the fully wrapped SSB−ssDNA complex.

On the basis of the SSB tetramer−ssDNA structure determined by X-ray crystallography (*6*), a molecule of $(dT)_{70}$ bound to the SSB tetramer in the fully wrapped $(SSB)_{65}$ binding mode should have its 5′- and 3′-ends located close to each other (see Figure 1). Therefore, if fluorescent probes (donor−acceptor pair) that can undergo fluorescence resonance energy transfer (FRET) when in close proximity are placed at the two ends of a ssDNA that is 65−70 nucleotides long, then an increase in the fluorescence of the acceptor fluorophore (upon exciting the donor fluorophore) should be observed upon formation of the fully wrapped SSB−$(dT)_{70}$ complex. To test this idea, we labeled $(dT)_{70}$ with hexachlorofluorescein (acceptor) at its 5′-end and placed a fluorescein (donor) fluorophore at different positions along the contour length of the $(dT)_{70}$. Using this series of constructs, we observed that the maximum FRET signal is observed when the dyes were placed at the 5′- and 3′-ends of the $(dT)_{70}$ (data not shown).

In the study presented here, we synthesized the ssDNA molecule, 5′-Cy5$(dT)_{65}$Cy3dT-3′, in which the fluorophore, Cy3 (donor), was covalently attached near the 3′-end of the DNA and the fluorophore, Cy5 (acceptor), was covalently attached to the 5′-end. This Cy3−Cy5 (donor−acceptor) FRET pair is well-characterized, with an R_0 value of ∼50−53 Å (*32*, *33*), and has been used in a number of FRET studies (*34*, *35*). Figure 8 shows the fluorescence emission spectra (515 nm excitation wavelength) of Cy5$(dT)_{65}$Cy3dT alone and in a 1:1 complex with the SSB tetramer in 1 M NaCl (buffer T, pH 8.1, 25.0 °C). An excitation wavelength of 515 nm excites the Cy3 donor, while no direct excitation of the Cy5 acceptor occurs at this wavelength. This was demonstrated by showing that no Cy5 fluorescence signal (667 nm maximum wavelength) was observed when a similar ssDNA molecule that contained only the Cy5 fluorophore was excited at 515 nm. The corrected spectra in Figure 8 show that when the Cy3 donor is excited at 515 nm, the Cy5 fluorescence (667 nm) of Cy5$(dT)_{65}$Cy3dT increases approximately 3-fold upon formation of the fully wrapped SSB−ssDNA complex, reflecting a significant FRET signal. However, we also note that a corresponding decrease in Cy3 fluorescence (565 nm) is not observed upon SSB binding, although a corresponding loss in Cy3 fluorescence is expected if the only effect on the Cy3 fluorescence signal were due to the loss of Cy3 fluorescence due to the transfer of energy to the Cy5 acceptor. In fact, a slight increase in Cy3 fluorescence is observed upon formation of the SSB−Cy5$(dT)_{65}$Cy3dT complex. This indicates that the SSB protein interacts with the Cy3 fluorophore, resulting in an increase in the quantum yield of the Cy3, which more than compensates for the decrease resulting from the FRET effect. The net result is a slight increase in the Cy3 fluorescence intensity. Consistent with this conclusion, independent equilibrium titration studies (in 2 M NaBr) of SSB binding to $(dT)_{70}$ labeled only with Cy3 have shown that the equilibrium binding constant is increased 10-fold by the presence of the Cy3 fluorophore (unpublished data). Hence, the Cy3 fluorophore does interact directly with the SSB protein, and this interaction increases the fluorescence quantum yield of the Cy3 fluorophore. Nonetheless, the fluorescence emission from Cy5 is only observed for a ssDNA molecule that is labeled with both Cy3 and Cy5 resulting from FRET due to the proximity of the two fluorophores upon formation of the fully wrapped SSB−ssDNA complex. Therefore, the Cy5 fluorescence emission can be used to monitor the formation of the fully wrapped complex.

A 2-fold further increase in SSB concentration (data not shown) does not result in any further changes to the fluorescence emission spectrum of the SSB−Cy5$(dT)_{65}$Cy3dT complex shown in Figure 8. This indicates that the SSB tetramer forms a fully wrapped 1:1 complex with the ssDNA at this high salt concentration (1 M NaCl), as expected from our previous studies of this complex (*2*, *10*, *25*), and does not form the $(SSB)_{35}$ binding mode in which two SSB tetramers can bind to a $(dT)_{70}$ molecule. However, at lower NaCl concentrations (20 mM NaCl), an $(SSB)_{35}$ complex can form in which 2 mol of SSB tetramer is bound to the same Cy5$(dT)_{65}$Cy3dT molecule at high [SSB]:[Cy5$(dT)_{65}$Cy3dT] ratios. Formation of this $(SSB)_{35}$ complex results in a lower Cy5 FRET signal than is observed for the fully wrapped 1:1 complex due to the increased distance between the Cy3 and Cy5 fluorophores within the $(SSB)_{35}$ complex (data not shown).

Two series of stopped-flow experiments were performed by mixing SSB with Cy5$(dT)_{65}$Cy3dT in 1 M NaCl (buffer T, pH 8.1, 25.0 °C). In one set of experiments, the Cy5 FRET signal was monitored upon mixing of Cy5$(dT)_{65}$Cy3dT (20 nM) with varying concentrations of an excess of SSB protein (see Figure 9A). In the second series of experiments, the SSB Trp fluorescence signal was monitored upon mixing

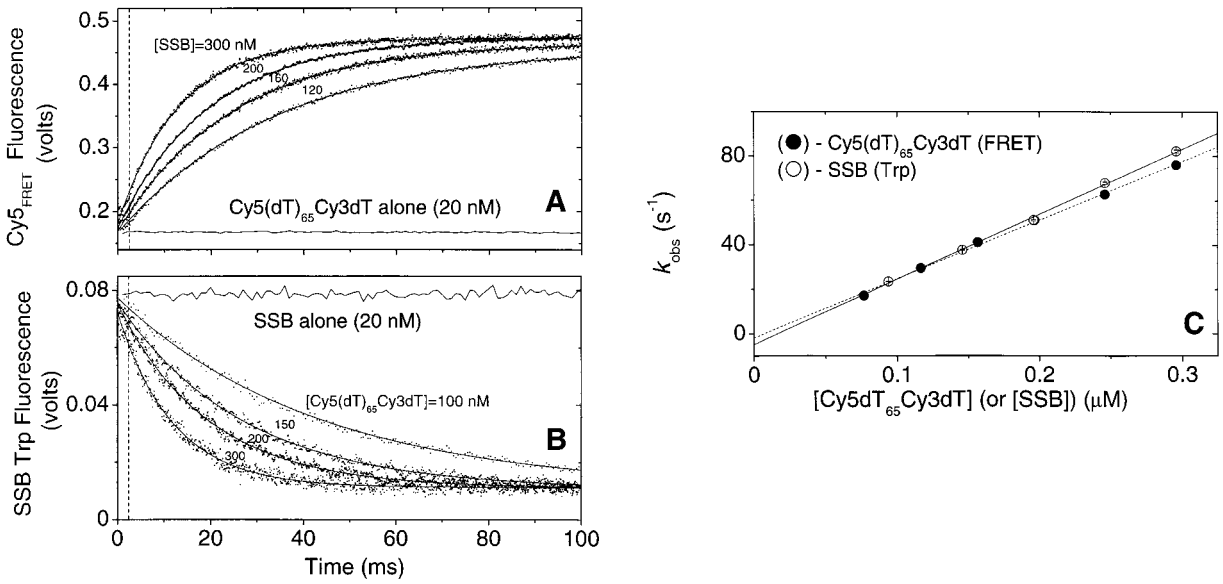

FIGURE 9: Comparisons of the kinetic time courses for SSB tetramer binding to $Cy5(dT)_{65}Cy3dT$ as monitored by the increase in Cy5 FRET and the decrease in SSB Trp fluorescence (1 M NaCl, buffer T, pH 8.1, 25 °C). (A) Stopped-flow time courses obtained by monitoring the Cy5 fluorescence ($\lambda_{ex} = 515$ nm) upon mixing $Cy5(dT)_{65}Cy3dT$ (20 nM) with increasing concentrations of SSB. (B) Stopped-flow time courses obtained by monitoring SSB Trp fluorescence ($\lambda_{ex} = 296$ nm) upon mixing SSB (20 nM tetramer) with increasing concentrations of $Cy5(dT)_{65}Cy3dT$. Solid lines represent the best fits of the traces to a single-exponential function using eq 1. As before, only data points to the right of the vertical dashed lines at 2.5 ms were used in the analyses. (C) Dependence on [SSB] of k_{obs} obtained from the fits shown in panel A (●; the dashed line is the linear least-squares line through the data) and dependence on $[Cy5(dT)_{65}Cy3dT]$ of k_{obs} obtained from the fits shown in panel B (○; the solid line is the linear least-squares line through the data).

SSB (20 nM) with an excess of the $Cy5(dT)_{65}Cy3dT$ DNA (see Figure 9B). In the first set of experiments (Cy5 FRET), the formation of the fully wrapped structure is monitored, whereas in the second set of experiments (Trp fluorescence), both binding and wrapping should be monitored. The data and results are shown in Figure 9 and Table 1.

The fluorescence time courses from both types of experiments are described very well by single-exponential decays, and these data were fit to eq 1 to obtain the decay constants, k_{obs} (see panels A and B of Figure 9). The dependencies of k_{obs} on $[SSB]_{tot}$ and $[Cy5(dT)_{65}Cy3dT]_{tot}$ obtained from these single-exponential fits are shown in Figure 9C. For both sets of experiments, k_{obs} is a linear function of $[SSB]_{tot}$ and $[Cy5(dT)_{65}Cy3dT]_{tot}$. Furthermore, with the possible exception of the experiments performed at the highest concentrations, the data are superimposable and described by the same linear dependence. The slopes of the two linear least-squares lines are identical within experimental uncertainty with the following values of $k_{1,app}$: $(2.9 \pm 0.1) \times 10^8$ and $(2.7 \pm 0.1) \times 10^8$ M^{-1} s^{-1}. These values of $k_{1,app}$ are the same as the values obtained under the same conditions using unlabeled $(dT)_{70}$ (see Table 1). The same values of $k_{1,app}$ were also determined upon direct fitting of Trp fluorescence traces (as well as FRET fluorescence traces) in experiments performed when $[SSB] \approx [Cy5dT_{65}Cy3dT]$ (see Table 1). Therefore, these experiments indicate that complete wrapping of the ssDNA around the SSB tetramer must occur much faster than the binding event (see Scheme 1), which is why the ssDNA binding and wrapping appear to occur simultaneously on the stopped-flow time scale.

Kinetics of $(dT)_{35}$ Binding to SSB in 0.2 M NaCl. The equilibrium binding data obtained previously for $(dT)_{35}$ binding to SSB monitored by tryptophan fluorescence quenching (*19*−*21*) and by ITC (*25*) show that two molecules of $(dT)_{35}$ can bind per SSB tetramer, although with a negative cooperativity that increases with decreasing salt concentration. At high concentrations of NaCl (>0.2 M), both macroscopic equilibrium binding constants ($K_{obs,1/35}$ and $K_{obs,2/35}$) decrease with increasing NaCl concentrations (*20*, *25*). We have used stopped-flow kinetics to compare the rates of SSB binding to $(dT)_{35}$ and $(dT)_{70}$ in the presence of 0.2 M NaCl (buffer T, pH 8.1, 25 °C) since the extent of wrapping around the SSB tetramer will differ for these different length oligodeoxynucleotides.

The stopped-flow SSB Trp fluorescence quenching time courses obtained upon mixing SSB (30 nM) with an excess of $(dT)_{35}$ are shown in Figure 10A. Under these conditions, two molecules of $(dT)_{35}$ can bind to each SSB tetramer at equilibrium. The time courses are well-described by the sum of two exponential phases, indicating that binding occurs in at least two steps (see Scheme 2). Two observed rates ($k_{obs,1}$ and $k_{obs,2}$) obtained from the double-exponential fits using eq 1 are plotted versus $[(dT)_{35}]_{tot}$ in Figure 10B. In the range of $(dT)_{35}$ concentrations that was examined, both $k_{obs,1}$ and $k_{obs,2}$ exhibit linear dependencies on $(dT)_{35}$ concentration and have negative intercepts. This suggests that the two phases reflect binding of the first and second molecules, respectively, of $(dT)_{35}$ to an SSB tetramer. Linear least-squares analyses of these data yield values of $(9.20 \pm 0.30) \times 10^8$ and $(1.03 \pm 0.04) \times 10^8$ M^{-1} s^{-1} for the apparent bimolecular rate constants, indicating that there is an approximately 10-fold difference between the bimolecular rate constants for binding of the first and second molecules of $(dT)_{35}$. This ~10-fold lower rate of binding for the second molecule of $(dT)_{35}$ likely reflects the same negative cooperativity that is observed at the equilibrium binding level. As in the case for SSB binding to $(dT)_{70}$, the negative intercepts in these linear plots reflect the fact that $k_{1,35}[P]_{tot} \gg k_{-1,35}$ and $k_{2,35}[P]_{tot} \gg k_{-2,35}$. From a comparison of $k_{1,35}$ and $k_{2,35}$ with the values of $K_{obs,1,35}$ ($>5.3 \times 10^9$ M^{-1}) and $K_{obs,2/35}$ (3.3×10^8 M^{-1}) obtained

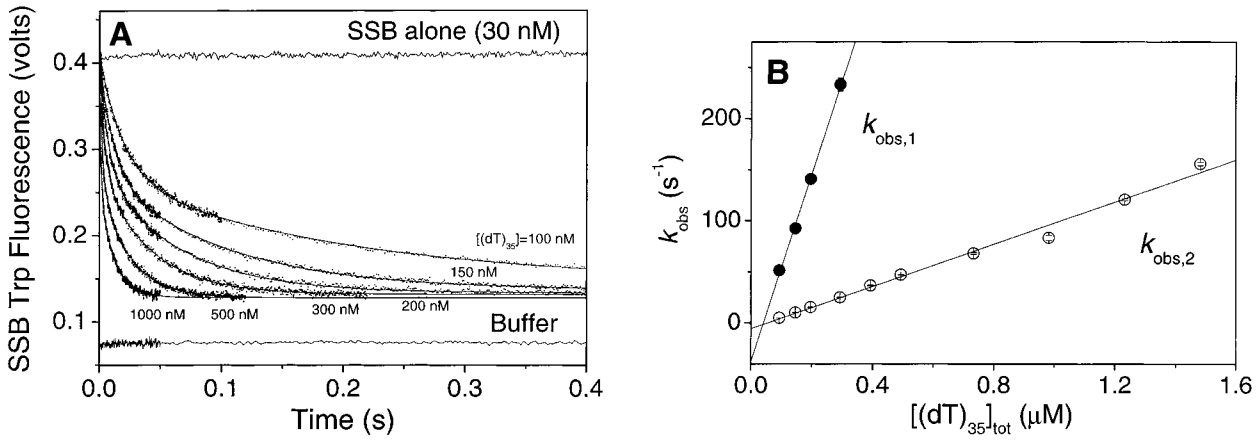

FIGURE 10: Stopped-flow kinetic time courses for the binding of $(dT)_{35}$ to the SSB tetramer. (A) SSB Trp fluorescence was monitored upon mixing SSB (30 nM tetramer) with varying concentrations of $[(dT)_{35}]$ (0.2 M NaCl, buffer T, pH 8.1, 25 °C). Solid lines are the nonlinear least-squares fits of the data to a double-exponential function (eq 1 with $n = 2$). (B) Observed rates for the first phase [$k_{obs,1}$ (●)] and the second phase [$k_{obs,2}$ (○)] are plotted as a function of total $(dT)_{35}$ concentration. Solid lines are the linear least-squares fits of the data yielding the following parameters: (●) $k_{1,35} = (9.20 \pm 0.03) \times 10^8$ s^{-1} M^{-1} (slope) and intercept $= -37.9 \pm 5.7$ s^{-1} for the dependence of $k_{obs,1}$ and (○) $k_{2,35} = (1.03 \pm 0.04) \times 10^8$ s^{-1} M^{-1} (slope) and intercept $= -5.5 \pm 2.9$ s^{-1} for the dependence of $k_{obs,2}$.

Scheme 2

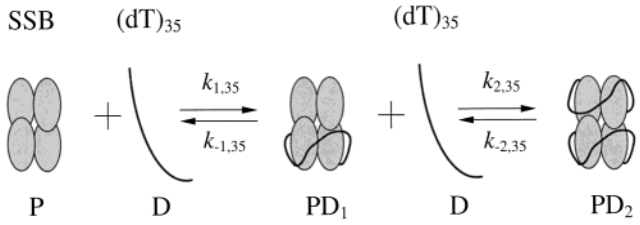

previously (*20*), it is clear that both of the apparent dissociation rate constants, $k_{-1,35}$ and $k_{-2,35}$, are expected to be ≤ 0.3 s^{-1}.

DISCUSSION

Due to the homotetrameric nature of the *E. coli* SSB protein and the fact that each subunit contains a ssDNA binding site (*27*, *36*), the SSB tetramer can bind single-stranded polynucleotides in a number of different binding modes that differ by the number of subunits that interact with the DNA and thus the extent of wrapping (for reviews, see refs *2* and *7*). The equilibrium properties and transitions among the different polynucleotide binding modes have been studied in detail. At high salt concentrations (>0.2 M monovalent salt, or in the presence of multivalent cations), the SSB tetramer can form a so-called $(SSB)_{65}$ mode in which all four subunits bind ~65 nucleotides of ssDNA to form a fully wrapped complex. However, at low monovalent salt concentrations (<10 mM NaCl), a so-called $(SSB)_{35}$ complex is favored in which the tetramer covers ~35 nucleotides, with the ssDNA forming interactions with approximately two subunits. When bound to ss-polynucleotides, the intertetramer cooperativity between SSB tetramers differs dramatically for these two binding modes (*15*). The $(SSB)_{35}$ binding mode appears to be able to form long protein clusters along the ssDNA polymer of the type that are assumed to be important for DNA replication, whereas the $(SSB)_{65}$ binding mode displays a much lower cooperativity of a different ("limited") type such that long clusters of tetramers are not observed, but are limited to forming dimers of tetramers.

The kinetics of DNA binding to and wrapping around the SSB tetramer has not been examined in as much detail. In fact, nearly all previous studies of the kinetics of *E. coli* SSB protein binding to ssDNA were performed before it was recognized that the SSB tetramer can bind to ssDNA in a number of different binding modes. In addition, most of the previous studies were carried out using either ss-polynucleotides that were polydisperse in length (*31*, *37*) or ss-oligodeoxynucleotides [e.g., $(dT)_8$, $(dT)_{16}$, or a mixture of $(dT)_{30-40}$] (*38*). The former studies with polynucleotides are complicated by the fact that SSB can bind these long ssDNAs in multiple modes, with the binding mode distribution depending on the solution conditions and protein binding density, whereas the latter studies used oligodeoxynucleotides that were too short to fully wrap around the tetramer. To gain an understanding of the kinetic mechanism of ssDNA binding to and wrapping around the SSB tetramer, we have examined the binding of ss-oligodeoxynucleotides to a single SSB tetramer, hence removing any complications due to intertetramer positive cooperativity that would exist if polynucleotides were used. We have used oligodeoxythymidylates of two lengths, $(dT)_{70}$, which is long enough to form a fully wrapped tetramer as depicted in Figure 1, and $(dT)_{35}$, to which the tetramer can bind and form a singly ligated complex, making approximately half the contacts, or a doubly ligated complex, which should be similar to the fully wrapped SSB−$(dT)_{70}$ complex. The final states of the SSB−ss-oligodeoxynucleotide complexes studied here are well-defined, and the thermodynamics of binding have been characterized in detail by fluorescence (*16*, *19*−*21*, *28*) and isothermal titration calorimetry (*25*, *39*, *40*, *41*).

We have examined the kinetics of SSB tetramer binding to $(dT)_{70}$ (buffer T, pH 8.1, 25.0 °C) at several monovalent salt (NaCl and NaBr) concentrations in the range from 0.2 to 2 M. Under these conditions, the final equilibrium complex consists of one molecule of $(dT)_{70}$ bound per SSB tetramer such that the ssDNA interacts with all four protein subunits. The stopped-flow kinetic time courses obtained by monitoring the quenching of SSB Trp fluorescence indicate that formation of the complex is very fast and is accompanied by a quenching of approximately 84−90% of the initial SSB Trp fluorescence, in good agreement with the extent of Trp fluorescence quenching observed for a fully wrapped SSB−

$(dT)_{70}$ complex at equilibrium under these conditions. Furthermore, under pseudo-first-order conditions {[$(dT)_{70}$)] ≫ [SSB]}, only a single-exponential time course is observed, suggesting that the reaction rate is limited by a single step.

The apparent bimolecular rate constant, $k_{1,app}$, for association of SSB with $(dT)_{70}$ is extremely high at low salt concentrations, being $9.1-9.5 \times 10^8$ M^{-1} s^{-1} at 0.2 M NaCl (see Table 1) and exceeding 10^9 M^{-1} s^{-1} at 20 mM NaCl (see Figure 6). The low-salt limiting value of $k_{1,app}$ [$(1.13 \pm 0.03) \times 10^9$ M^{-1} s^{-1}] is very close to that expected for a diffusion-limited association reaction. Using the expression developed by Berg et al. (*42*) for nonspecific association of a protein with any site within the DNA domain, a diffusion-limited association rate constant k_a of 1.65×10^9 M^{-1} s^{-1} can be calculated using the parameters for a 70-nucleotide ssDNA (*31*), although this calculation neglects orientational and electrostatic effects. The $k_{1,35}$ value of $(9.20 \pm 0.30) \times 10^8$ M^{-1} s^{-1} for the association of one molecule of $(dT)_{35}$ to the SSB tetramer (0.2 M NaCl, buffer T, pH 8.1, 25 °C) is nearly identical to the value measured for $(dT)_{70}$ [$(9.47 \pm 0.30) \times 10^8$ M^{-1} s^{-1}] under the same conditions.

The values of the bimolecular association rate constants obtained here for SSB binding to $(dT)_{70}$ and $(dT)_{35}$ are quite similar to the values reported for SSB binding to ss-polynucleotides. k_a values of 2.4×10^9 M^{-1} (polynucleotide) s^{-1} and 1.1×10^9 M^{-1} s^{-1} have been reported for SSB binding to poly(dT) at 0.2 and 0.95 M NaCl, respectively (*37*). A k_a value of 2.5×10^9 M^{-1} (polynucleotide) s^{-1} has been reported for SSB binding to poly(U) at 0.2 M NaCl (*31*), and these show the same general decrease as a function of NaCl concentration.

Krauss et al. (*38*) studied the kinetics of SSB binding to a series of short oligodeoxythymidylates using temperature jump approaches, by monitoring the quenching of SSB Trp fluorescence upon binding (20 mM phosphate, pH 7.4, 0.2 M KCl, 8 °C). They measured apparent bimolecular association rate constants of 7×10^7, 5×10^7, and 3×10^8 M^{-1} (oligo) s^{-1} for the binding of $(dT)_8$, $(dT)_{16}$, and $(dT)_{30-40}$, respectively. The value of k_a reported for $(dT)_{30-40}$ binding to SSB (*38*) is between our values of 9×10^8 and 1×10^8 M^{-1} (oligo) s^{-1} for the binding of the first and second molecules of $(dT)_{35}$, respectively, although we note that the solution conditions and temperature used for the two sets of experiments are different.

The rate constants for dissociation of the SSB−$(dT)_{70}$ and SSB−$(dT)_{35}$ complexes are too small to be measured accurately with the approaches described here under the conditions used in our experiments. In general, we can give only upper estimates for $k_{-1,app}$ of <2 s^{-1} based on the negative intercepts of the plots of k_{obs} versus [DNA] and for $k_{-1,app}$ of <0.1 s^{-1} from the direct fitting of the time courses obtained at equimolar SSB and $(dT)_{70}$ concentrations (see Table 1). However, we have obtained more accurate estimates based on the results of competition experiments (data in preparation).

Wrapping of $(dT)_{70}$ around the SSB Tetramer Is Fast Relative to the Initial Binding Step. Our stopped-flow experiments performed under pseudo-first-order conditions ([DNA] ≫ [SSB]) demonstrate that binding of $(dT)_{70}$ to SSB is rapid and follows a single-exponential time course with ~90% quenching of the SSB Trp fluorescence and an apparent bimolecular association rate constant, $k_{1,app}$ approaching 10^9 M^{-1} s^{-1} at low salt concentrations. Therefore, the binding reaction can be described by a single, nearly diffusion controlled step, but the final SSB−$(dT)_{70}$ complex has the ssDNA interacting with all four subunits and fully wrapped around the SSB tetramer. This suggests that the rate of the DNA wrapping step is very fast, relative to the initial binding step, and that it is not possible to separate the binding and wrapping steps (see Scheme 1) based solely on the kinetic data from monitoring Trp fluorescence quenching. Therefore, to further probe the kinetics of the wrapping step(s), we performed kinetic experiments using $(dT)_{66}$ labeled at the 3′- and 5′-ends with the fluorophores, Cy3 (donor) and Cy5 (acceptor), respectively, which can serve as the donor−acceptor pair in a FRET experiment. The 3′- and 5′-ends of an oligodeoxynucleotide of ~65−70 nucleotides should be in close proximity when bound to the SSB tetramer in a fully wrapped complex, based on the model developed from the SSB tetramer−ssDNA X-ray crystallographic structure (*6*) (see Figure 1). Therefore, the time course of formation of a fully wrapped SSB−$(dT)_{66}$ complex can be monitored by the change in the FRET signal from the Cy3−Cy5 pair.

The kinetic time courses obtained by monitoring the Cy5 FRET signal from Cy5$(dT)_{65}$Cy3dT (buffer T, pH 8.1, 1 M NaCl, 25 °C) are identical, within error, to the time courses obtained using the same DNA, but monitoring SSB Trp fluorescence quenching (see Figure 9 and Table 1). Each time course is characterized by a single-exponential decay, indicating that the binding and wrapping steps (see Scheme 1) cannot be separated, and that the rate of the second step (wrapping) is very fast relative to the rate of the first (binding) step. In other words, although in general the reaction in Scheme 1 will be characterized by two eigenvalues (λ_1 and λ_2), and thus two relaxation phases, only one phase is observed in our stopped-flow experiments. The other phase, which is too fast to observe in the stopped-flow instrument, is dominated by the rate constants governing the second wrapping step.

Solving the system of differential equations for Scheme 1 (for the conditions, [D] ≫ [P]) and applying the square-root approximation (*43*) for the second eigenvalue ($\lambda_2 = k_{obs}$), one obtains the expression in eq 12

$$\lambda_2 = \frac{k_1[D](k_2 + k_{-2}) + k_{-1}k_{-2}}{k_1[D] + k_{-1} + k_2 + k_{-2}} \qquad (12)$$

In general, eq 12 predicts a hyperbolic dependence of k_{obs} on [$(dT)_{70}$] (D) with an approximately linear behavior at low D concentrations, and a limiting (plateau) value at high [D] concentrations corresponding to $k_2 + k_{-2}$. In our studies, we observe a linear dependence of k_{obs} on [D], with no indication of curvature up to the maximum rates that were experimentally accessible [$k_{obs,max} = 700$ s^{-1} (at 100 nM SSB)]. Therefore, the wrapping rate constants ($k_2 + k_{-2}$) must be >700 s^{-1}.

Under all of the conditions of the experiments reported here, k_{-1} in Scheme 1 is expected to be very low, and thus, $k_{-1} \ll k_2$. After application of this constraint and in the limit of low ssDNA concentration, eq 12 simplifies to eq 13.

$$k_{obs} = \frac{k_{-1}k_{-2}}{k_2 + k_{-2}} + k_1[D] \qquad (13)$$

Therefore, the slope of a plot of k_{obs} versus [ssDNA] yields the association rate constant, k_1 in Scheme 1, and the intercept defines an apparent dissociation rate constant [$k_{-1,app} = k_{-1}k_{-2}/(k_2 + k_{-2})$]. Furthermore, if $k_2 \gg k_{-2}$, then the apparent dissociation rate constant simplifies further to $k_{-1,app} = k_{-1}k_{-2}/k_2$, and thus is expected to be very small. For instance, if $k_{-1} = k_{-2} = 1\ s^{-1}$ and $k_2 > 1000\ s^{-1}$, then $k_{-1,app} < 10^{-3}\ s^{-1}$. The estimates of $k_{-1,app}$ from direct fitting of the traces to eq 8a give values in the range of $0.003-0.01\ s^{-1}$ (see column 7 of Table 1). Finally, we note that if $k_{-2} \gg k_2$, then eq 13 simplifies still further so that $k_{obs} = k_{-1} + k_1[D]$.

It is interesting to compare the lower limit for the unimolecular rate constant for the wrapping step ($>700\ s^{-1}$) with the apparent bimolecular rate constant for binding of a second molecule of $(dT)_{35}$ to the SSB tetramer ($1 \times 10^8\ M^{-1}\ s^{-1}$). These results indicate that a $(dT)_{35}$ concentration of >7 μM would be needed to achieve a rate for the binding of the second $(dT)_{35}$ molecule that approaches the rate of wrapping. Therefore, the increased local concentration of the ssDNA to be wrapped, when it is part of the longer $(dT)_{70}$, contributes to the high rate of wrapping.

Dependence of $k_{1,app}$ on the Monovalent Salt Concentration and Type. Due to the polyanionic nature of nucleic acids, the equilibrium binding constants, K_{obs}, for most protein−nucleic acid interactions are quite sensitive to the bulk salt concentration, with K_{obs} generally decreasing with increasing salt concentration. The origins of these salt dependencies can be quite complex, with contributions from differential binding of ions (cations and/or anions) to the protein−DNA complex, relative to the free DNA and/or protein. Generally, there is a net displacement of ions upon formation of the protein−nucleic acid complex, and thus, the equilibrium association constant decreases with increasing salt concentration. This has been well-documented in studies of the binding of *E. coli* SSB protein to ss-polynucleotides (*18*) and ss-oligodeoxynucleotides (*20*, *21*). In the case of *E. coli* SSB protein, the salt dependence of the equilibrium constant has contributions from a net cation displacement from the ssDNA, but also from a net anion displacement from the protein (*18*, *44*). There are also contributions from cation binding by the SSB−ssDNA complex. These ion binding phenomena will also result in a salt sensitivity of the kinetic rate constants, with the dissociation rate constant generally being more sensitive to salt concentration than the association rate constant (for reviews, see refs *31* and *45*).

In general, there are two possible explanations for the dependence of the association rate constant, $k_{1,app}$, on monovalent salt concentration (NaCl and NaBr). The first is a general electrostatic screening effect. Such an effect should be relatively small and dependent only upon the ionic strength of the solution and thus independent of ion type (*31*). Since our results (Figure 6) demonstrate a specific effect of anion type (Cl^- vs Br^-), this indicates that a simple screening effect is not the only factor contributing to the salt effect on $k_{1,app}$. The second possibility is that the ions that can bind both to the ssDNA (cations) and to the SSB protein (cations and/or anions) can compete for binding of the protein and the DNA, respectively. Our previous studies of the equilibrium binding of SSB to ssDNA (*18*, *20*, *21*, *25*, *44*) demonstrate that there is a net release of monovalent anions from the SSB protein as well as a net release of monovalent cations, primarily from the DNA, upon formation of the SSB−ssDNA complex. Some cation binding to the SSB protein also accompanies the formation of the SSB−DNA complex (*18*). From a series of detailed studies of the effects of monovalent salt concentration and type and the linkage to pH, Overman and Lohman (*44*) have concluded that there are approximately five anion binding sites on the SSB protein that are perturbed upon formation of an SSB complex with poly(U) in the $(SSB)_{65}$ binding mode.

The following analysis is based on the assumption that the observed dependence of $k_{1,app}$ on salt concentration results from the competitive binding of anions to the SSB protein, although, as discussed above, there is also certainly some contribution due to cation binding to the DNA and/or protein as well. For this reason, the following analysis should be viewed only as a first approximation for an explanation of the salt effect on $k_{1,app}$. We assume that the binding of monovalent anions (Cl^- and/or Br^-) to "n" independent and identical sites on the protein competes directly for binding of the ssDNA as described by the scheme in eqs 14

$$P + D \underset{k_{-1,0}}{\overset{k_{1,0}}{\rightleftharpoons}} PD$$

$$P + A \underset{k_{-A}}{\overset{k_A}{\rightleftharpoons}} PA + A \underset{k_{-A}}{\overset{k_A}{\rightleftharpoons}} PA_2 + A \ldots \underset{k_{-A}}{\overset{k_A}{\rightleftharpoons}} PA_n \quad (14)$$

where P, D, and A represent SSB protein, ssDNA, and anion, respectively. We have also assumed that anion binding to the SSB protein can be treated as a rapid equilibrium reaction (i.e., $k_A[A]$, $k_{-A} \gg k_{1,0}[D]$, $k_{-1,0}$) where $K_A = k_A/k_{-A}$. These assumptions lead to the expression in eq 15 for the dependence of $k_{1,app}$ on salt concentration.

$$k_{1,app} = \frac{k_{1,0}}{(1 + K_A A)^n} \quad (15)$$

Taking the logarithm of both sides yields eq 16

$$\log k_{1,app} = \log k_{1,0} - n \log(1 + K_A[A]) \quad (16)$$

which we have used to analyze the data in Figure 6. Since the parameters K_A and n are highly correlated, they cannot be determined independently from analysis of the data. However, on the basis of the studies of Overman and Lohman (*44*), we have fixed n equal to 5. In that case, fitting of the data shown in Figure 6 to eq 16 yields the following: $k_{1,0} = (1.17 \pm 0.09) \times 10^9\ M^{-1}\ s^{-1}$ and $K_{Cl} = 0.30 \pm 0.02\ M^{-1}$ for NaCl and $k_{1,0} = (1.02 \pm 0.13) \times 10^9\ M^{-1}\ s^{-1}$ and $K_{Br} = 0.49 \pm 0.04\ M^{-1}$ for NaBr. If the actual value of n is lower (higher) than 5, the values of K_A will increase (decrease). However, the low-salt limiting value of k_1 obtained from this analysis is relatively insensitive to the model that is used. We note that the values of K_A obtained from this simplified approach are lower than the values of K_{Cl} ($7.5 \pm 1\ M^{-1}$) and K_{Br} ($21 \pm 3\ M^{-1}$) obtained from the global analysis of equilibrium data for SSB binding to poly(U) in its $(SSB)_{65}$ binding mode (*44*). This likely reflects our neglect of the effects due to cation release or uptake that we know does occur in the reaction. Therefore, the values of the anion binding constants obtained from our fitting of the data to eq 16 should be viewed only as fitting parameters. However, the low values of K_A

estimated above are consistent with results from our previous studies of the effects of monovalent salt concentration and type on the observed enthalpy of binding for the SSB−$(dT)_{70}$ interaction, as measured by isothermal titration calorimetry (ITC) (*25*).

Implications for the Interaction of SSB Tetramers with ss-Polynucleotides. Our experiments, as well as those from previous studies (*37*, *38*), indicate that the rate of complete dissociation of SSB from a single-stranded DNA even as short as $(dT)_{35}$ is quite low ($\ll 1\ s^{-1}$) even at the highest NaCl concentration used in our studies (2 M). Therefore, when an SSB tetramer is bound to a ss-polynucleotide that is long enough to fully wrap around the tetramer (≥ 70 nucleotides), the probability is low that a region of ssDNA corresponding to as many as 35 nucleotides will "peel off" of the SSB tetramer and expose two SSB subunits. However, previous studies by Krauss et al. (*38*) have measured a rate constant of 40 s^{-1} (pH 7.4, 200 mM KCl, 8 °C) for dissociation of a shorter oligodeoxynucleotide, $(dT)_{16}$, from the SSB tetramer. This rate will likely be higher at the higher temperature used in our studies. Therefore, once a fully wrapped SSB tetramer is formed, regions corresponding to ~16 nucleotides, or one subunit's worth of ssDNA, could potentially dissociate on that time scale, making one subunit transiently unoccupied at a rate of $\geq 40\ s^{-1}$. Of course, this region of ssDNA would reassociate rapidly, based on the results reported here. As first suggested by Romer et al. (*37*), this opens the possibility that an isolated SSB tetramer bound to a ss-polynucleotide could undergo a one-dimensional translocation along the ss-polynucleotide using a "rolling" mechanism. In this scenario, a short region of ssDNA that transiently dissociates from only one subunit can be replaced with a region of ssDNA from the other side of the tetramer. In this way, a random walk of the SSB tetramer could occur in steps of ~16 nucleotides**.** Whether such a translocation process is biologically functional remains to be examined.

ACKNOWLEDGMENT

We thank Dr. G. Waksman for preparing Figure 1 and T. Ho for synthesis and purification of the oligodeoxynucleotides used in this study.

REFERENCES

1. Meyer, R. R., and Laine, P. S. (1990) *Microbiol. Rev. 54*, 342−380.
2. Lohman, T. M., and Ferrari, M. E. (1994) *Annu. Rev. Biochem. 63*, 527−570.
3. Chase, J. W., and Williams, K. R. (1986) *Annu. Rev. Biochem. 55*, 103−136.
4. Kelman, Z., Yuzhakov, A., Andjelkovic, J., and O'Donnell, M. (1998) *EMBO J. 17*, 2436−2449.
5. Raghunathan, S., Ricard, C. S., Lohman, T. M., and Waksman, G. (1997) *Proc. Natl. Acad. Sci. U.S.A. 94*, 6652−6657.
6. Raghunathan, S., Kozlov, A. G., Lohman, T. M., and Waksman, G. (2000) *Nat. Struct. Biol. 7*, 648−652.
7. Lohman, T. M., and Bujalowski, W. (1990) in *The Biology of Nonspecific DNA-Protein Interactions* (Revzin, A., Ed.) pp 131−170, CRC Press, Boca Raton, FL.
8. Greipel, J., Urbanke, C., and Maass, G. (1989) in *Protein-Nucleic Acid Interaction* (Saenger, W., and Heinemann, U., Eds.) pp 61−86, CRC Press, Boca Raton, FL.
9. Lohman, T. M., and Overman, L. B. (1985) *J. Biol. Chem. 260*, 3594−3603.
10. Bujalowski, W., and Lohman, T. M. (1986) *Biochemistry 25*, 7799−7802.
11. Bujalowski, W., Overman, L. B., and Lohman, T. M. (1988) *J. Biol. Chem. 263*, 4629−4640.
12. Chrysogelos, S., and Griffith, J. (1982) *Proc. Natl. Acad. Sci. U.S.A. 79*, 5803−5807.
13. Griffith, J. D., Harris, L. D., and Register, J., III (1984) *Cold Spring Harbor Symp. Quant. Biol. 49*, 553−559.
14. Wei, T.-F., Bujalowski, W., and Lohman, T. M. (1992) *Biochemistry 31*, 6166−6174.
15. Lohman, T. M., Overman, L. B., and Datta, S. (1986) *J. Mol. Biol. 187*, 603−615.
16. Ferrari, M. E., Bujalowski, W., and Lohman, T. M. (1994) *J. Mol. Biol. 236*, 106−123.
17. Bujalowski, W., and Lohman, T. M. (1987) *J. Mol. Biol. 195*, 897−907.
18. Overman, L. B., Bujalowski, W., and Lohman, T. M. (1988) *Biochemistry 27*, 456−471.
19. Lohman, T. M., and Bujalowski, W. (1988) *Biochemistry 27*, 2260−2265.
20. Bujalowski, W., and Lohman, T. M. (1989) *J. Mol. Biol. 207*, 269−288.
21. Bujalowski, W., and Lohman, T. M. (1989) *J. Mol. Biol. 207*, 249−268.
22. Webster, G., Genschel, J., Curth, U., Urbanke, C., Kang, C., and Hilgenfeld, R. (1997) *FEBS Lett. 411*, 313−316.
23. Yang, C., Curth, U., Urbanke, C., and Kang, C. (1997) *Nat. Struct. Biol. 4*, 153−157.
24. Williams, K. R., Spicer, E. K., LoPresti, M. B., Guggenheimer, R. A., and Chase, J. W. (1983) *J. Biol. Chem. 258*, 3346−3355.
25. Kozlov, A. G., and Lohman, T. M. (1998) *J. Mol. Biol. 278*, 997−1012.
26. Lohman, T. M., Green, J. M., and Beyer, S. (1986) *Biochemistry 25*, 21−25.
27. Bujalowski, W., and Lohman, T. M. (1991) *J. Biol. Chem. 266*, 1616−1626.
28. Ferrari, M. E., and Lohman, T. M. (1994) *Biochemistry 33*, 12896−12910.
29. Kowalczykowski, S. C., Lonberg, N., Newport, J. W., and von Hippel, P. H. (1981) *J. Mol. Biol. 145*, 75−104.
30. Erickson, J., Goldstein, B., Holowka, D., and Baird, B. (1987) *Biophys. J. 52*, 657−662.
31. Lohman, T. M. (1986) in *CRC Critical Reviews in Biochemistry*, pp 191−245, CRC Press, Boca Raton, FL.
32. Bastiaens, P. I. H., and Jovin, T. M. (1996) *Proc. Natl. Acad. Sci. U.S.A. 93*, 8407−8412.
33. Deniz, A. A., Dahan, M., Grunwell, J. R., Ha, T., Faulhaber, A. E., Chemla, D. S., Weiss, S., and Schultz, P. G. (1999) *Proc. Natl. Acad. Sci. U.S.A. 96*, 3670−3675.
34. Zhuang, X., Bartley, L. E., Babcock, H. P., Russell, R., Ha, T., Herschlag, D., and Chu, S. (2000) *Science 288*, 2048−2051.
35. Cheng, W., Hsieh, J., Brendza, K. M., and Lohman, T. M. (2001) *J. Mol. Biol. 310*, 327−350.
36. Bujalowski, W., and Lohman, T. M. (1991) *J. Mol. Biol. 217*, 63−74.
37. Romer, R., Schomburg, U., Krauss, G., and Maass, G. (1984) *Biochemistry 23*, 6132−6137.
38. Krauss, G., Sindermann, H., Schomburg, U., and Maass, G. (1981) *Biochemistry 20*, 5346−5352.
39. Lohman, T. M., Overman, L. B., Ferrari, M. E., and Kozlov, A. G. (1996) *Biochemistry 35*, 5272−5279.
40. Kozlov, A. G., and Lohman, T. M. (1999) *Biochemistry 38*, 7388−7391.
41. Kozlov, A. G., and Lohman, T. M. (2000) *Proteins: Struct., Funct., Genet. 4* (Suppl.), 8−22.
42. Berg, O. G., Winter, R. B., and von Hippel, P. H. (1981) *Biochemistry 20*, 6929−6948.
43. Johnson, K. A. (1986) *Methods Enzymol. 134*, 677−702.
44. Overman, L. B., and Lohman, T. M. (1994) *J. Mol. Biol. 236*, 165−178.
45. Record, M. T., Jr., Ha, J.-H., and Fisher, M. A. (1991) in *Methods in Enzymology* (Sauer, R. T., Ed.) pp 291−343, Academic Press, New York.

BI020122Z